






Sorghum root epigenetic landscape during limiting phosphorus conditions

Nicholas Gladman¹  | Barbara Hufnagel²  | Michael Regulski¹ | Zhigang Liu³ | Xiaofei Wang¹ | Kapeel Chougule¹ | Leon Kochian³  | Jurandir Magalhães⁴  | Doreen Ware^{1,5} 

¹Cold Spring Harbor Laboratory, Cold Spring Harbor, New York, USA

²Centre National de la Recherche Scientifique, Montpellier, Languedoc-Roussillon, France

³Global Institute for Food Security, University of Saskatchewan, Saskatoon, Canada

⁴Embrapa Milho e Sorgo, Sete Lagoas, Brazil

⁵U.S. Department of Agriculture-Agricultural Research Service, NEA Robert W. Holley Center for Agriculture and Health, Cornell University, Ithaca, New York, USA

Correspondence

Doreen Ware, U.S. Department of Agriculture-Agricultural Research Service, NEA Robert W. Holley Center for Agriculture and Health, Cornell University, Ithaca, NY 14853, USA.
Email: ware@csnl.edu

Funding information

National Council for Scientific and Technological Development (CNPq); Fundação de Amparo à Pesquisa do Estado de Minas Gerais (FAPEMIG); Embrapa Macroprogram; United States Department of Agriculture, Grant/Award Number: 8062-21000-041-00D; Global institute for Food Security, University of Saskatchewan; Canada Excellence Research Chairs (CERC), Government of Canada

Abstract

Efficient acquisition and use of available phosphorus from the soil is crucial for plant growth, development, and yield. With an ever-increasing acreage of croplands with suboptimal available soil phosphorus, genetic improvement of sorghum germplasm for enhanced phosphorus acquisition from soil is crucial to increasing agricultural output and reducing inputs, while confronted with a growing world population and uncertain climate. *Sorghum bicolor* is a globally important commodity for food, fodder, and forage. Known for robust tolerance to heat, drought, and other abiotic stresses, its capacity for optimal phosphorus use efficiency (PUE) is still being investigated for optimized root system architectures (RSA). Whilst a few RSA-influencing genes have been identified in sorghum and other grasses, the epigenetic impact on expression and tissue-specific activation of candidate PUE genes remains elusive. Here, we present transcriptomic, epigenetic, and regulatory network profiling of RSA modulation in the BTx623 sorghum background in response to limiting phosphorus (LP) conditions. We show that during LP, sorghum RSA is remodeled to increase root length and surface area, likely enhancing its ability to acquire P. Global DNA 5-methylcytosine and H3K4 and H3K27 trimethylation levels decrease in response to LP, while H3K4me3 peaks and DNA hypomethylated regions contain recognition motifs of numerous developmental and nutrient responsive transcription factors that display disparate expression patterns between different root tissues (primary root apex, elongation zone, and lateral root apex).

KEYWORDS

chromatin modification, DNA methylation, histone marks, histone methylation, phosphorus efficiency, phosphorus responsive genes, RNA seq, root system architecture; root system remodeling; phosphorous deficiency

In response to low P, epigenetic and transcriptional changes stimulate lateral root growth in *Sorghum bicolor* BTx623, increasing the root surface area for enhanced “mining” of P from the soil.

This is an open access article under the terms of the [Creative Commons Attribution](https://creativecommons.org/licenses/by/4.0/) License, which permits use, distribution and reproduction in any medium, provided the original work is properly cited.

© 2022 The Authors. Plant Direct published by American Society of Plant Biologists and the Society for Experimental Biology and John Wiley & Sons Ltd.

1 | INTRODUCTION

Sorghum [*Sorghum bicolor* (L.) Moench] was domesticated in northern Africa ~6000 years ago (de Wet & Huckabay, 1967; Dillon et al., 2007). A C₄ grass crop with notable tolerance to drought, heat, and high-salt conditions, sorghum is a top-10 global crop in terms of acreage use. It also serves as a useful model for crop research due to its completely sequenced compact genome (~730 Mb) (Cooper et al., 2019; McCormick et al., 2018; Paterson et al., 2009) and similarity to crops with larger genomes where repetitive sequences are more prevalent, such as in maize.

Adequate supply of phosphorus (P), which, as one of the most three most widely used crop fertilizers (N, P, and K), is limited by finite P reserves worldwide (Cordell & White, 2013), limits many cropping systems throughout the world (Calderón-Vázquez et al., 2009). Over 30% of the global cropland are phosphorus deficient (MacDonald et al., 2011), due mainly to P fixation, which is the tendency of phosphate anions to be tightly bound to the surface of soil clay minerals (López-Arredondo et al., 2014). This has been exacerbated because high quality rock phosphate reserves are localized to and extracted from a small number of countries (Cordell et al., 2009). While steady advances in yield have been made across multiple crop species (<http://www.fao.org/faostat/en/#data>), more will have to be done on the germplasm side to increase overall cropping system PUE.

In recent years, genetic variation in root system architecture (RSA) has been recognized to play an important role in the efficient acquisition of mineral nutrients from the soil, especially with regard to root phosphorus acquisition (Bellini et al., 2014; Lynch, 2011). Sorghum adaptation to low-P conditions in the soil is largely governed by P acquisition efficiency with higher root surface area and reduced root diameter acting in concert to enhance P uptake and grain yield (Bernardino et al., 2019; Hufnagel et al., 2014). In fact, a generalized response to low soil phosphorus (LP) involve alterations in root architecture such as those leading to longer and thinner lateral roots, more shallow lateral root angles, and increased root hair production, which all can act to enhance the plant's ability to mine this diffusion-limited nutrient from the soil (López-Bucio et al., 2002; Péret et al., 2014; Schulze et al., 2006). While there is both intra- and inter-species variation in RSA that are associated with P efficiency (defined in this study as improved crop yield on low P soils) (Bayuelo-Jiménez et al., 2011; Miller et al., 2003), most grasses can show similar structural responses to LP. The molecular mechanisms underlying morphological changes in the root system likely involve a number of signaling cascades (Barros et al., 2020; Hu et al., 2011; Hufnagel et al., 2014; Park et al., 2014; Thibaud et al., 2010) that can be under epigenetic control (Yong-Villalobos et al., 2015) as well as numerous transcription factors (Devaiah et al., 2007; Zhou et al., 2008). Aside from hormone responses in auxin, cytokinin, ethylene, and jasmonic acid pathways (Khan et al., 2016; Li et al., 2012; López-Bucio et al., 2002; Nguyen et al., 2013; Thibaud et al., 2010), there are also notable changes in the epigenetic landscape of the genome that influences transcription factor binding and subsequent *cis*-regulation of gene expression

(Chen et al., 2018; Dai et al., 2012; Deng et al., 2016; Nguyen et al., 2013; Smith et al., 2010).

Genetic variation leads to sorghum adaptation to abiotic stress conditions (Dombia et al., 1993, 1998; Hufnagel et al., 2014; Leiser et al., 2014), and there has been recent progress with evincing the genetic components underlying sorghum adaptation to soils with low P availability (Bernardino et al., 2019; Hufnagel et al., 2014; Leiser et al., 2014). Specifically, after the identification of the important serine/threonine receptor kinase PSTOL1 in rice (Gamuyao et al., 2012), sorghum PSTOL1 homologs were identified and shown to enhance P acquisition and grain yield under low-P conditions (Hufnagel et al., 2014).

However, much of the epigenetic contribution to nutrient response regulatory networks remains nebulous. Some advancements have been made into regulatory network construction incorporating transcriptomic and regulatory epigenetic regions, such as enhancers, in the related crops of rice and maize (Deng et al., 2016; Shi et al., 2014; West et al., 2014; Zhou et al., 2020), along with investigations of other genes that play roles in plant response to a low phosphorus environment which possibly could be involved in P efficiency (Li et al., 2012; Mora-Macias et al., 2017).

2 | RESULTS

2.1 | Sorghum root system responses to low vs sufficient phosphorus supply

Figure 1 shows representative root images of BTx623 plants grown in our 2D root imaging system. As described in detail in the Materials and Methods, these individual growth systems contain the roots in acrylic chambers, which allow for unrestricted growth of the root systems while maintaining their 2-dimensional RSA and allow for high resolution imaging and analysis of the individual root systems at high throughput. The plants depicted in Figure 1 are representative of the growth response for five replicates grown under sufficient P (SP; 200- μ M phosphate) or low P (LP; 2.5- μ M phosphate), which were imaged at 7, 10, and 14 days after transfer to the SP and LP nutrient solution. Several results are highlighted here: (1) Although seedlings of some sorghum cultivars can produce several seminal roots from the sorghum embryo, for the root systems on all five replicate BTx623 plants, only one seminal root was produced, as is shown for one of the five replicate plants in Figure 1, and all of the lateral roots emerge from that seminal root. (2) In response to growth on LP nutrient solution, a significant enhancement in lateral root growth is observed.

The root trait data for BTx623 root systems grown on SP and LP nutrient solution for 7, 10, and 14 DAT are presented in Table 1. It is clear that LP conditions trigger a general increase in both root surface and volume, favoring proliferation of finer roots. The most dramatic low P-induced responses were increases in total root length and root volume (an approximation of root biomass) which is dominated by increases in lateral root growth. A statistically significant decrease in root diameter is also seen by 10 and 14 DAT of growth in LP vs. SP

FIGURE 1 Sorghum root system architecture (RSA) under sufficient (SP) and limiting phosphorus (LP). BTx623 seedlings were germinated for 4 days then transferred to hydroponic solutions containing either SP (200 μM) or LP (2.5 μM) nutrient media and grown for an additional 7, 10, or 14 days. Compared with SP conditions, LP stimulates more lateralization of the RSA in addition to deeper root growth through elongation of the apex and intermediate root zones

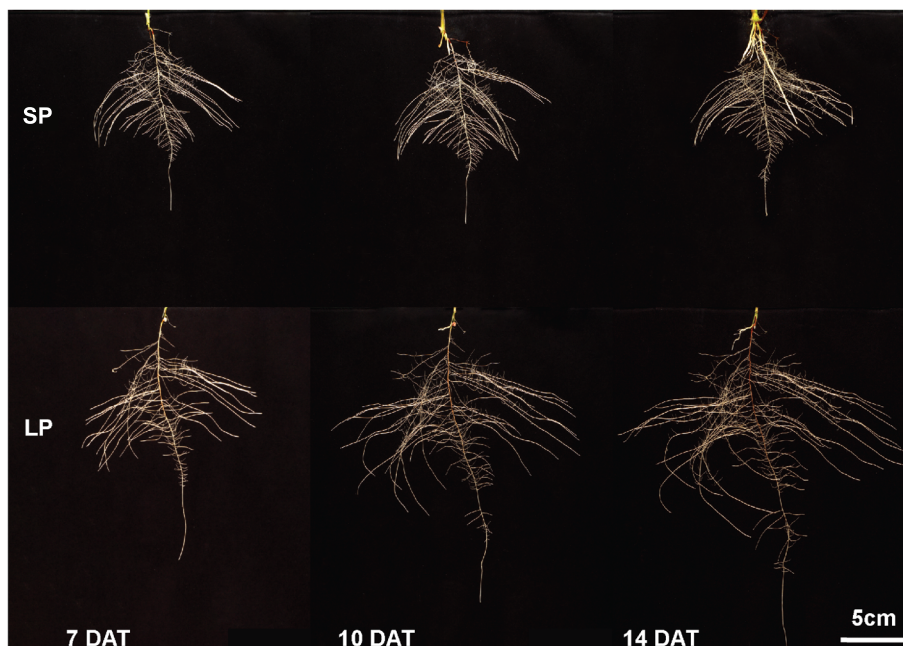


TABLE 1 Root system growth and architecture traits quantified for BTx623 grown in nutrient media for 7, 10, and 14 days after transplanting (DAT) under sufficient phosphorus (SP: 200 μM) and low phosphorus (LP: 2.5 μM) conditions

Trait	Average root diameter (cm)	Primary root length (cm)	Root system width (cm) ^a	Convex hull area (cm ²) ^b	Root system surface area (cm ²)	Total root system length (cm)	Total root system volume (cm ³)
7 DAT							
SP	.033 \pm .0004	13.3 \pm .4*	11.1 \pm .5	94 \pm 4*	33 \pm 2	324 \pm 16	0.31 \pm 0.01
LP	.032 \pm .0004	16.4 \pm 1.1	12.2 \pm 1.0	129 \pm 12	37 \pm 3	361 \pm 25	0.33 \pm 0.02
10 DAT							
SP	.033 \pm .0005*	13.6 \pm .5*	1.4 \pm 0.3*	96 \pm 4*	37 \pm 2*	361 \pm 21*	0.36 \pm 0.02
LP	.032 \pm .0001	19.1 \pm 1.2	14.9 \pm 1.4	188 \pm 22	58 \pm 7	581 \pm 68	0.51 \pm 0.06
14 DAT							
SP	.036 \pm .0012*	13.7 \pm .4*	1.5 \pm .5*	96 \pm 4*	43 \pm 4*	386 \pm 26*	0.48 \pm 0.07
LP	.031 \pm .0004	22.7 \pm 1.5	18.8 \pm 1.5	283 \pm 31	87 \pm 13	906 \pm 135	0.74 \pm 0.11

Note: Data shown are the means \pm SE for 5 replicates. Asterisk indicates the significance of differences ($P < .05$) between the P treatments, as determined by Student's *t*-test.

^aRoot system width is the maximum width of the entire root system.

^bConvex hull area is the area of the smallest convex polygon that encloses all of the set of points that define a specific 2D root system image.

conditions, consistent with the tendency observed at 7 DAT. All of these trait changes are consistent with known alterations in the root system triggered by low P conditions to more effectively explore a greater soil volume and thus more effectively acquire phosphate anions from soils with low P availability.

2.2 | Root system transcriptional responses to low phosphorus

To understand the molecular response to LP, a transcriptomic analysis that was performed on the seminal primary root apex (first 2 cm),

the seminal primary root elongation zone (2–4 cm from root tip), and the root apices of the lateral roots (first 2 cm) reveals that the low P induction of sorghum homologs of phosphorus starvation induced (PSI) genes was greatest in the lateral root apices (Figure 2a). Based on a gene ontology (GO) analysis within the lateral root apex, genes that displayed an expression change of twofold or greater in low phosphorus-grown plants were associated with a number of processes, including different P-related metabolic and signaling pathways, protein phosphorylation, plant response to changes in mineral nutrient availability, lipid modification, and metabolism (Table 2). Other general P-responsive changes in gene expression in the three root regions studied included increased decreased

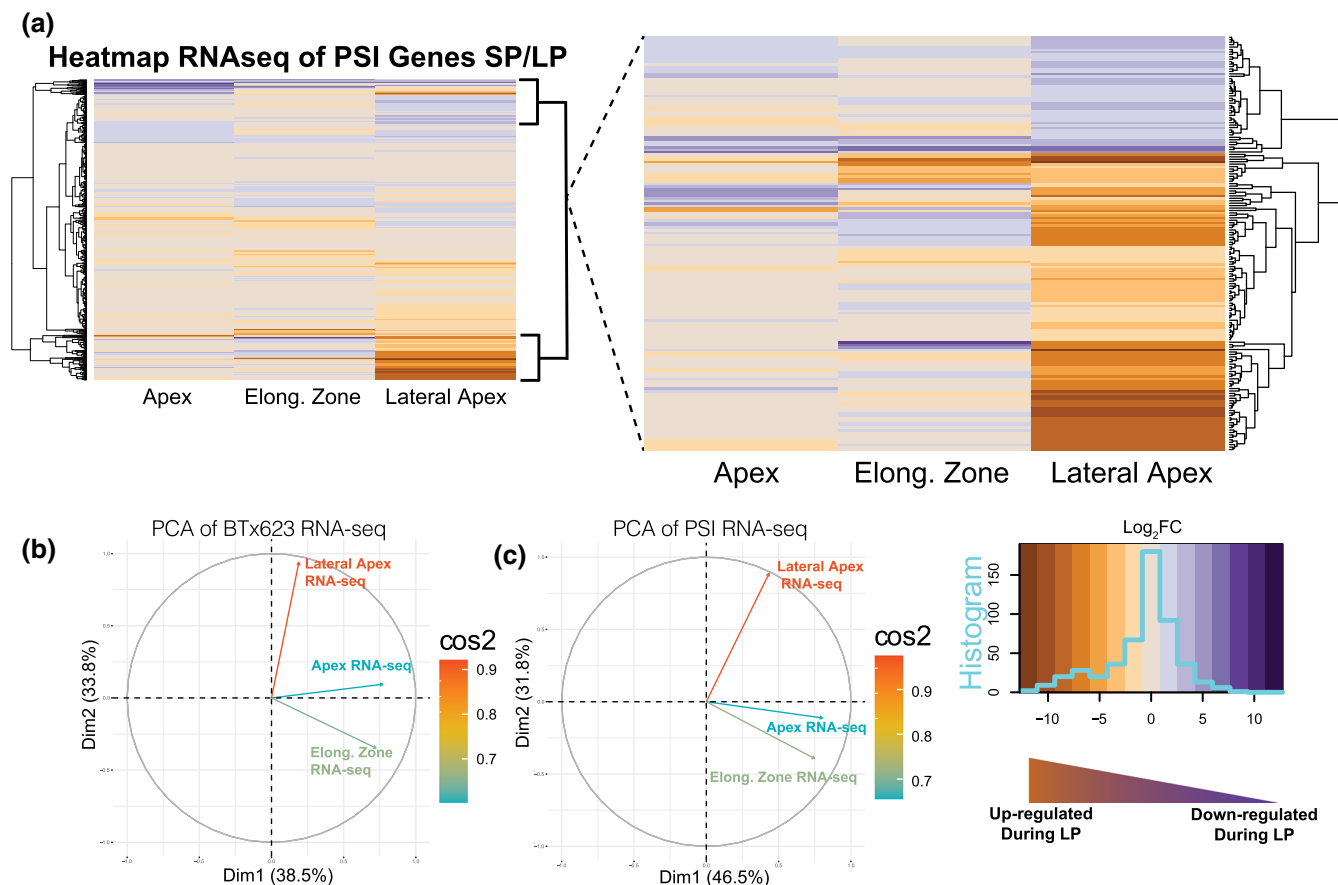


FIGURE 2 (a) Heatmap of all sorghum PSI gene orthologs with their root tissue RNA-seq profiles (smaller inset) and an expanded selection of highly differentially expressed PSI genes that shows that most of these genes are concentrated in the lateral root apex. The heatmap legend (lower left of panel) displays the frequency distribution (histogram - cyan trace) of expression of individual genes across the entire range of \log_2 fold change expression values. See Data S1 for topmost up- and down-regulated PSI genes. (b) PCA analysis of gene expression data with eigenvectors for different root regions, and (c) PCA analysis showing contribution of all PSI genes; importance of contribution is displayed as \cos^2

expression of genes involved in metabolic processes, as well as post-transcriptional and translational regulation within the seminal root apex. Also observed was increased expression of genes involved with synthesis of terpenoids and isoprenoids and repression of genes involved in RNA processing and modification, translation and regulation of gene expression in the seminal root subapical region (root elongation zone).

Upon inspecting distinct genes families, several well-known PSI genes were strongly upregulated in response to low P in the lateral root apices (Data S1 and S2). Many of these PSI transcripts belong to transporters, metabolic, and transcription factor family genes, and for these genes, in general their largest change in expression in response to low P was in the lateral root apex. To determine if a particular root region or gene family was responsible for the greatest variation within the transcriptomic data, a principal component analysis (PCA) was performed against the RNA-seq expression data for all BTx623 genes as well as for specific gene families (families associated with PSI, metabolic pathways, transcription factor families, etc.). No specific gene family was found to be clustered in the PCA, but gene expression in the lateral root apex displayed a noticeable

difference in correlation compared with either the root apex or root elongation zone based on their PCA eigenvectors direction and intensity (Figure 2b,c). This indicates a stronger transcriptional correlation between the root apex and subapical regions versus the lateral root regions with regards to low P induced changes in gene expression.

When evaluating subsets of other notable gene families, such as transcription factors and specifically the DNA binding domains of TF families involved in plant stress responses, such as AP2, WRKY, NAC, bZIP and B3, the lateral root apex displays a larger number of genes that also exhibit a greater up-regulation of P deficiency response genes compared with either the seminal root apex and the seminal root sub-apical regions. The later regions display either negligible or a greater number of P responsive down-regulated genes. A GO analysis of these transcription factor gene families that are strongly up-regulated (twofold expression or greater) in the lateral root regions shows an enrichment of auxin-activated signaling pathway genes (GO:0009734), whereas the down-regulated genes in the root apex are enriched for response to chitin (GO:0010200) and abscisic acid (ABA)-activated signaling pathway (GO:0009738), as well as the

**TABLE 2** Gene ontology enrichment of up-regulated genes with 2-fold expression or higher during LP conditions

Enriched GO terms in seminal root apex in response to LP			
GO biological process complete	Fold enrichment	Raw P value	FDR
Posttranscriptional regulation of gene expression (GO:0010608)	0.38	8.85E-06	6.19E-03
Positive regulation of protein metabolic process (GO:0051247)	0.38	8.70E-05	4.73E-02
Positive regulation of cellular protein metabolic process (GO:0032270)	0.36	6.78E-05	4.15E-02
Regulation of translation (GO:0006417)	0.23	7.03E-08	5.74E-05
Regulation of cellular amide metabolic process (GO:0034248)	0.23	4.99E-08	4.89E-05
Positive regulation of translation (GO:0045727)	0.04	1.54E-09	2.51E-06
Positive regulation of cellular amide metabolic process (GO:0034250)	0.04	1.54E-09	1.89E-06
Positive regulation of cytoplasmic translation (GO:2000767)	<0.01	1.04E-09	5.09E-06
Regulation of cytoplasmic translation (GO:2000765)	<0.01	1.04E-09	2.54E-06
Enriched GO terms in seminal subapical root region in response to LP			
GO biological process complete	Fold enrichment	Raw P value	FDR
Terpenoid biosynthetic process (GO:0016114)	2.04	3.23E-04	2.08E-02
Terpenoid metabolic process (GO:0006721)	1.9	5.83E-04	3.52E-02
Isoprenoid biosynthetic process (GO:0008299)	1.86	4.07E-04	2.55E-02
Isoprenoid metabolic process (GO:0006720)	1.78	2.79E-04	1.87E-02
Lipid metabolic process (GO:0006629)	1.3	3.17E-04	2.07E-02
Oxidation-reduction process (GO:0055114)	1.29	1.80E-07	2.52E-05
Enriched GO terms in lateral root apex in response to LP			
GO biological process complete	Fold enrichment	Raw P value	FDR
Response to nutrient levels (GO:0031667)	2.06	7.87E-04	4.94E-02
Phosphatidylinositol metabolic process (GO:0046488)	1.92	4.69E-04	3.02E-02
Glycerophospholipid metabolic process (GO:0006650)	1.8	1.56E-04	1.14E-02
Lipid modification (GO:0030258)	1.78	7.56E-04	4.81E-02
Small molecule catabolic process (GO:0044282)	1.71	1.11E-04	8.95E-03
DNA repair (GO:0006281)	1.68	1.00E-06	1.14E-04
Nucleic acid phosphodiester bond hydrolysis (GO:0090305)	1.49	4.57E-04	2.98E-02
Chromosome organization (GO:0051276)	1.45	8.70E-05	7.22E-03
RNA processing (GO:0006396)	1.33	1.23E-04	9.45E-03
Phosphorus metabolic process (GO:0006793)	1.32	3.14E-12	7.68E-10
Protein phosphorylation (GO:0006468)	1.29	2.90E-06	3.09E-04
Aromatic compound biosynthetic process (GO:0019438)	1.29	4.18E-04	2.80E-02
Organic cyclic compound biosynthetic process (GO:1901362)	1.28	3.90E-04	2.73E-02
Cellular nitrogen compound metabolic process (GO:0034641)	1.28	1.47E-11	3.28E-09
Organic substance biosynthetic process (GO:1901576)	1.17	7.94E-05	6.70E-03

Note: Fold enrichment = \log_2 gene expression on LP/gene expression on SP. Seminal Root Apex is the first 2 cm of the primary seminal root. Seminal subapical root region is the region located 2–4 cm behind the primary seminal root tip. Lateral root apex is the first 2 cm of the lateral root.

auxin-activated signaling pathway (GO:0009734). The strongly down-regulated WRKY transcription factors that are a part of the canonical PSI genes are paralogs involved in the salicylic acid pathway

and had association with fungal and chitin-responsive pathways (SORBI_3002G202800 and SORBI_3002G202700), displaying potential overlap of biotic and abiotic stress responsive pathways.

2.3 | DNA and histone methylation profile throughout the sorghum genome

To further understand the changes chromatin accessibility during LP conditions, ChIP-seq profiling and Bisulphite sequencing was performed. ChIP-seq Histone 3 (H3) lysine trimethylation showed distinctive signaling at different regions throughout the sorghum genome in the intergenic and genic space. H3K27me3 (repressive) and H3K4me3 (activation) marks had similar averaged global coverage nearby and within genic regions (Figure 3a). However, there was a drop (~50%) in H3K4me3 enrichment within the TSS, genic, and 5' prime UTR regions under LP conditions compared with SP. When interrogating intergenic regions, H3K4me3 enrichment increased by ~50% in response to LP growth conditions compared with SP, whereas K27me3 enrichment remained mostly unchanged under either phosphorus

growth treatment in the intergenic space (Figure 3b). Clustering analysis revealed that H3K4 trimethylation can be grouped into three primary *k*-means clusters: upstream, from >3,000 bp to the transcriptional start site (TSS), genic, and downstream/non-specific (Figure 3c,d). The H3K27 trimethylation *k*-means clusters cover genic, downstream (from transcriptional end site [TES] to >-3000 bp), and upstream/non-specific regions. In agreement with the enrichment observations, the heatmap analysis indicates that both the H3K4me3 and H3K27me3 signals appear to decrease across all regions under low phosphorus, with K4me3 decreasing noticeably more than K27me3. The heatmap analysis stops at 3 Kb upstream or downstream of the TSS and TES, respectively. So, the increased enrichment of the H3K4me3 in intergenic spaces under LP conditions (Figure 3a) must originate from further away than these margins, suggesting a role of enhancer elements or more distant promoter-binding locations.

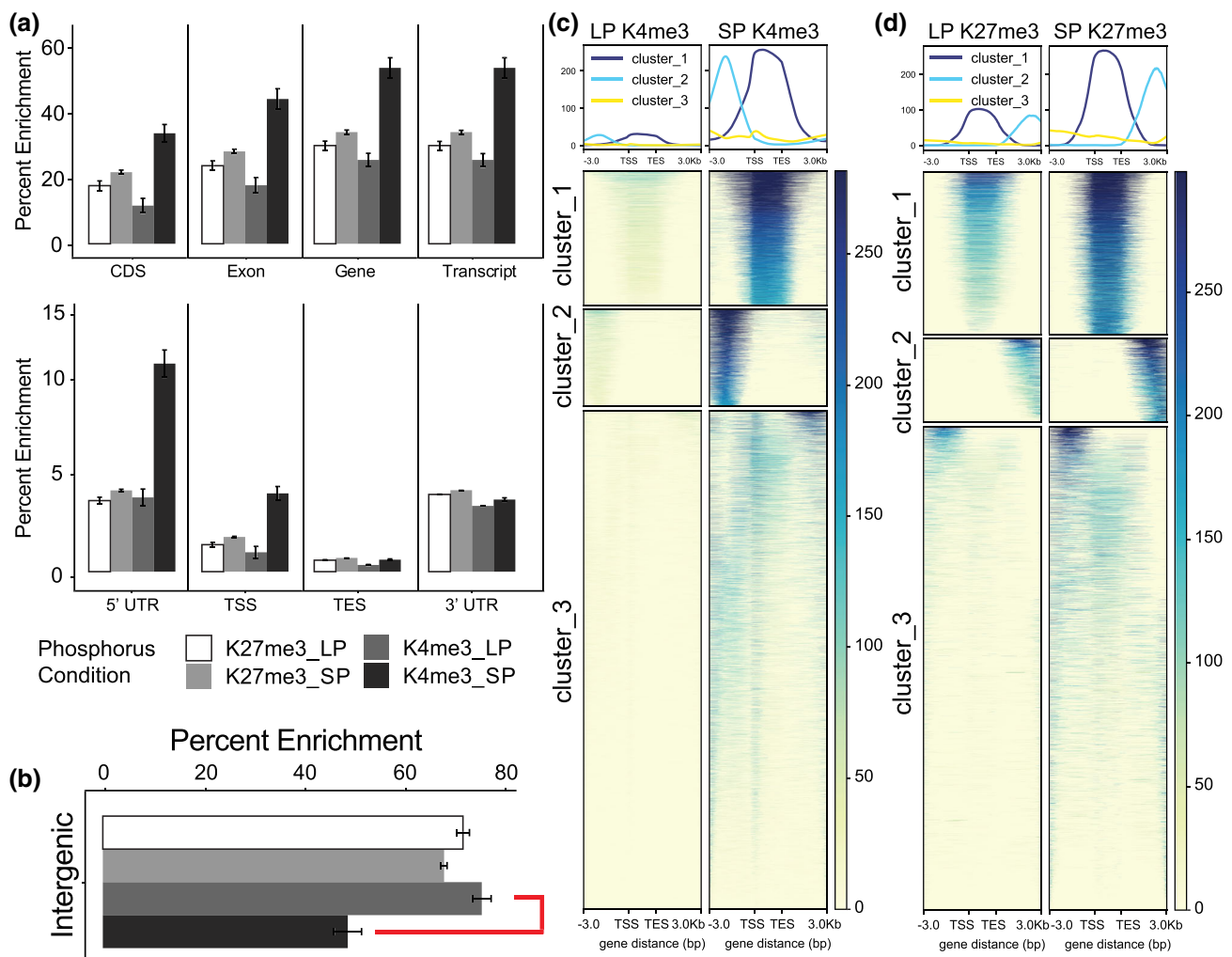


FIGURE 3 Epigenetic profiles of BTx623 whole root systems under normal and limiting phosphorus. (a) Global enrichment profiles of sorghum H3K27me3 and H3K4me3 across gene model components. (b) Global enrichment profile of K4me3 and K27me3 epigenetic marks across intergenic space during LP and SP. (c) Global heatmap and profile graphs of H3K27 and H3K4 trimethylation around gene models. K-means analysis generated three major clusters that roughly segregate methylation occurrences to genic, upstream, and/or downstream regions during normal and LP conditions

Sequence motif analysis revealed both shared and discrete DNA-binding motifs for both K27 and K4 histone methylation peaks, with certain motifs specific for growth on SP conditions and others specific for LP conditions (Figure 4). The recognition sequence for the APETALA2/ethylene-responsive element binding protein (AP2/EREB) transcription factors was enriched in both K4me3 and K27me3 peaks. While the DNA-binding sequence recognized by AP2/EREB family proteins was detected, the exact position weight matrices between P conditions varied. This could suggest that either a subset of AP2/EREBs are being regulated in response to P starvation based on their precise *cis*-binding motif or it could be reflective of a broad recognition profile for the AP2/EREB transcription factors. Other multiple transcription factor recognition-binding motifs were present upon inspection of the K4

and K27 methylation footprints. These included, but were not limited to, Trihelix, WRKY, NLP, NAC, ABI3, BZIP, and B3-domain containing TF families.

Bisulphite sequencing revealed that global DNA methylation (5-methylcytosine) enrichment levels remained mostly unchanged from SP to LP conditions across averaged genic or intergenic regions (Figure 5a,b) and decreased globally over genic regions, in line with previous observations for actively transcribed loci. DNA methylation levels were enriched the most in intergenic and transcribed regions and the least at the start and stop codon positions and at the three and five prime UTRs. DNA methylation was lower in exon regions compared with entire genes and transcripts, indicating increased methylation at the intron and non-coding gene space. Differential CG methylation in response to growth on LP conditions was the

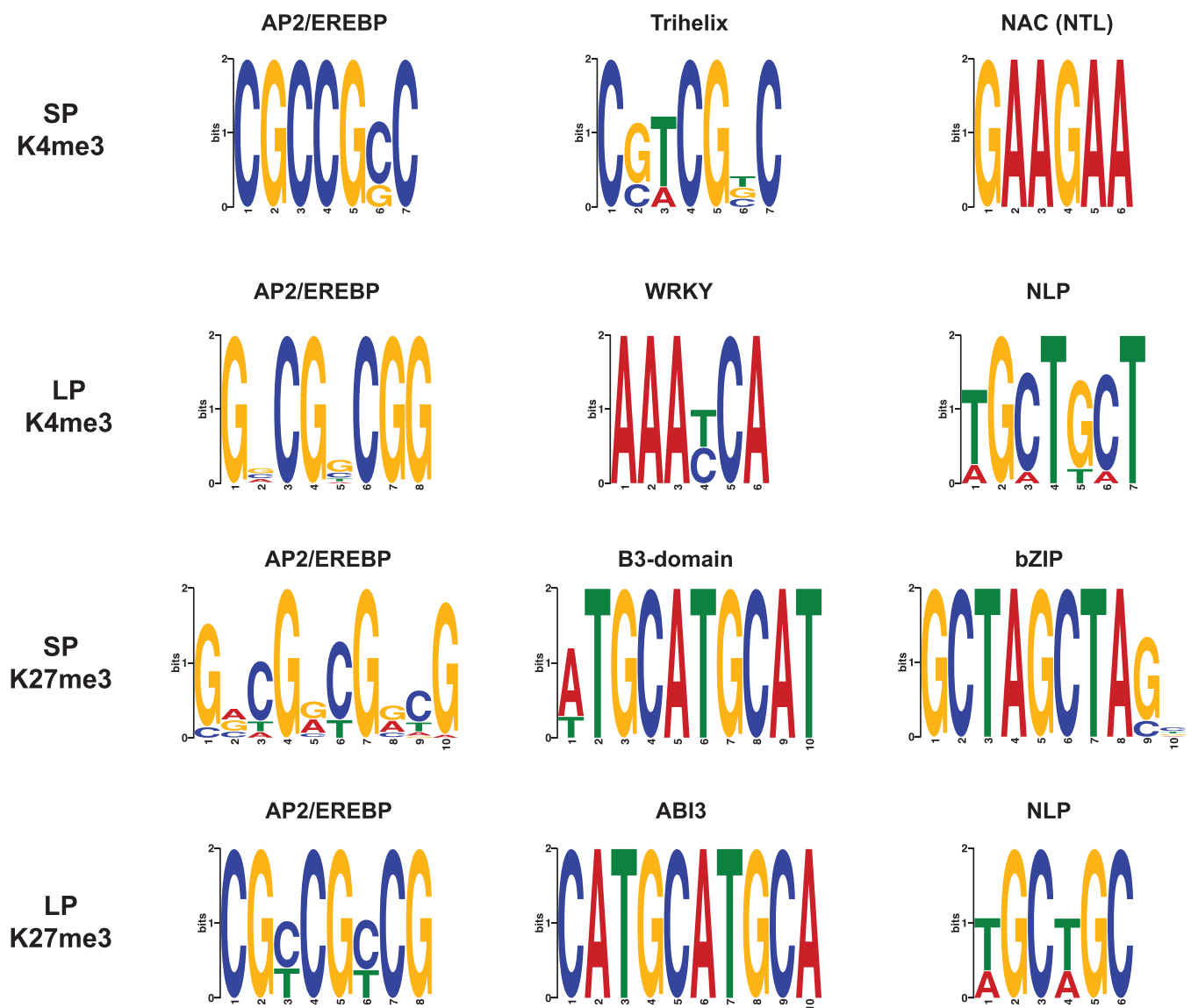


FIGURE 4 DNA binding motif enrichment analysis. Global MEME motif analysis of the 100 bp flanking sequences from K27me3 and K4me3 peaks during SP and LP conditions. All motifs were detected using the ANR method in the MEME suite program with minimum significance threshold of $e < .01$ or less

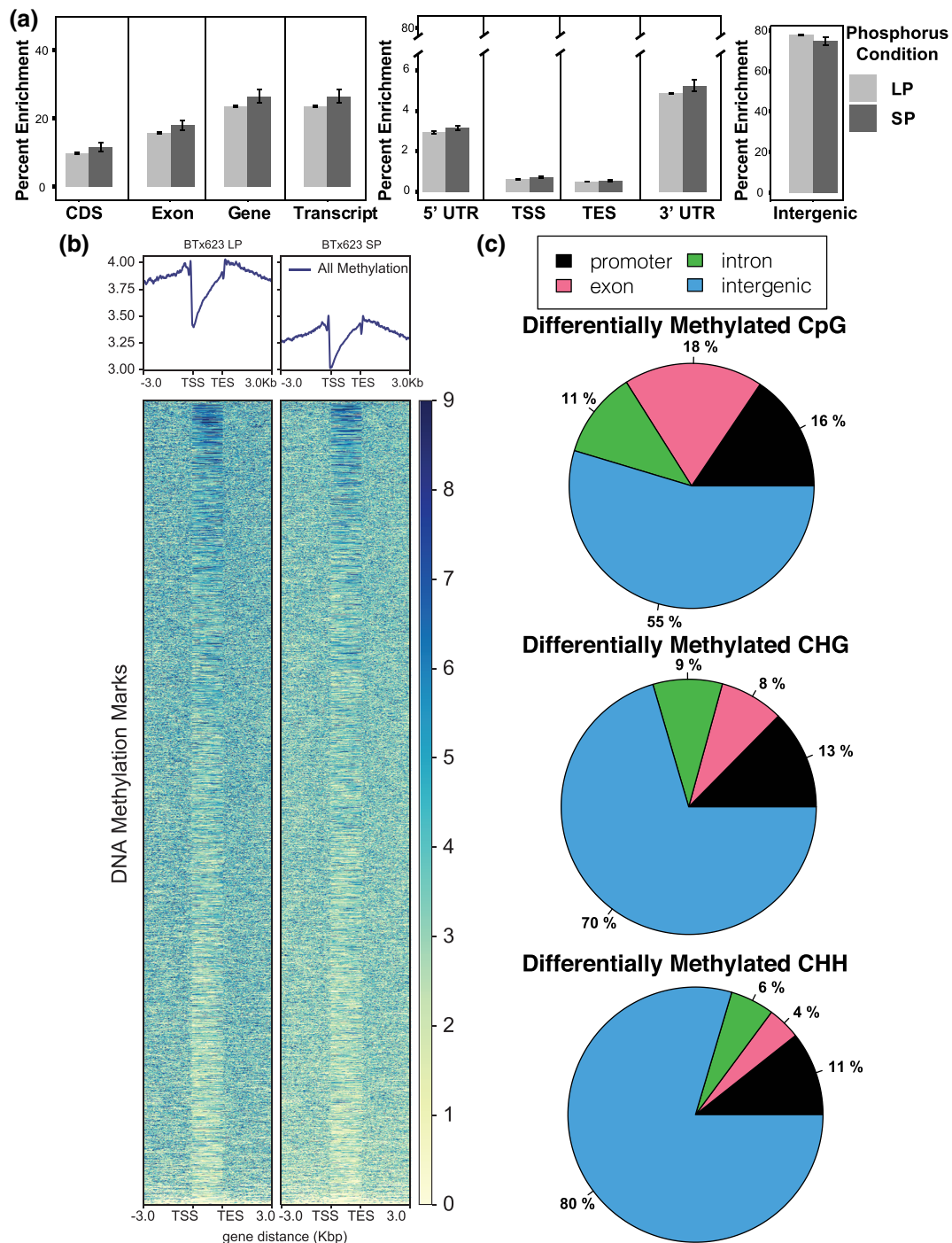


FIGURE 5 BTx623 global DNA methylation profile. (a) Global enrichment profiles of DNA methylation (BS = CG, CHG, and CHH) across gene model components during LP and SP conditions. (b) Heat map of 5-methylcytosine methylation across gene models in limiting (LP) and sufficient (SP) phosphorus. (c) Differentially DNA methylation (hypermethylated or hypomethylated) changes over promoter, exon, intron, and intergenic sequences in LP conditions compared with SP. Almost 100% of differential CHH methylation is hypomethylation

predominant form of differentially methylated regions (DMRs) and was more common at surrounding gene elements (promoters, exons, and introns) than either CHG or CHH methylation (Figures 5c and 6). Most of the CHG and CHH differential methylation (70–80%) was localized to the intergenic space (Figure 6b,c). CG hypomethylation is more common across the genome and specifically at genic and promoter

regions; hypomethylation is also the most common form of CHG DMR, but such changes were fairly similar at genic and promoter regions when compared with hypermethylation (Figure 6b,c). Notably, almost 100% of the statistically detected differential CHH methylation was hypomethylation. Motif analysis of regions surrounding differentially methylated CG marks were found to be enriched for

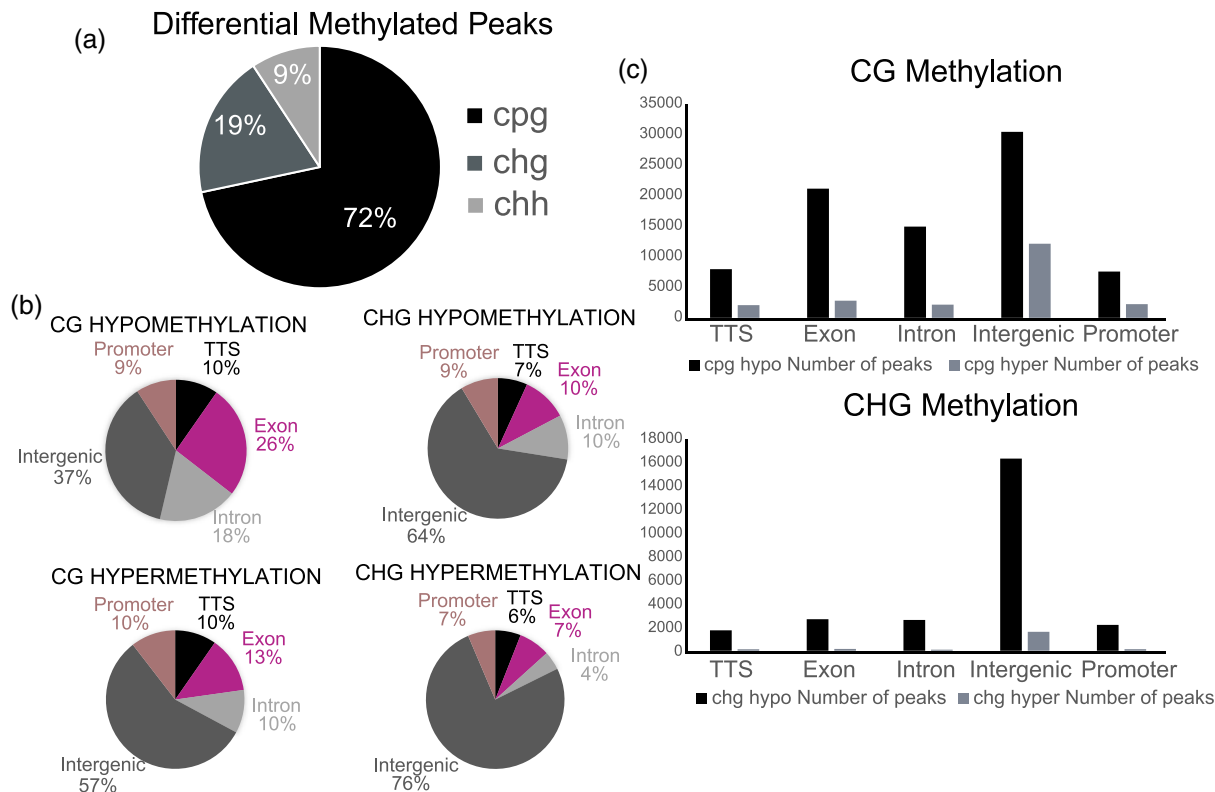


FIGURE 6 Differential DNA methylation regions in BTx623 (a) breakdown of all differentially methylated peaks (regions) by CG, CHG, and CHH in the BTx623 genome under LP growth conditions compared with SP growth. (b) Gene model breakdown of CG and CHG hypermethylation and hypomethylation in LP grown plants compared with SP. CHH DMRs are ~100% hypomethylated in roots of LP-grown plants. (c) Total number of CG and CHG DMRs by hypo- and hypermethylation by genomic location

AP2/EREB, WRKY, NLP, TCP, bZIP, C2H2, BZR, trihelix, and NAC family transcription factor binding sites (Figure S1). Additionally, CHG marks were enriched for AP2/EREB, WRKY, NLP, TCP, E2F-like, and LOB (Lateral Organ Boundary) transcription factors (Figure S2). DNA surrounding hypomethylated CHH loci were enriched for AP2/EREB, WRKY, NLP, TCP, and NAC transcription factor binding sites, amongst others (Figure S3).

The global change in histone trimethylation can also be observed by taking the ratio of K4 and K27 marks in the genic, 1000 and 5000 bp upstream bins and seeing how their frequency distribution changes (Figure S4). Across all intervals during growth on LP, the K4/K27 ratio distribution shrinks to a narrower range of values (specifically a lower ratio of K4 to K27) when compared with SP, suggesting that one or both marks are becoming less common and/or more consolidated across the epigenome in response to P limiting conditions.

Upon analysis of selected transcription factor gene families identified from the MEME analysis above and presented in Figure 5, it was determined that subgroups within these gene families display strong up- or down-regulation of expression in response to LP conditions (Figure S5). Specifically, a number of NAC, B3-domain containing, bZIP, WKRY, and AP2 transcription factors showed strong upregulation in the lateral root apices, and to a lesser extent in the primary root regions.

2.4 | Phosphorus responsive regulatory networks

To visualize complex interactions and contributions during root responses to LP growth conditions, protein-protein interaction networks were generated using the STRING database. The gene nodes were then filtered to reduce the network down to those genes that had associated K4me3 peaks; the gene nodes were then colored to correspond to their expression at lateral root regions. This phosphate responsive root gene regulatory network (GRN) was organized in a hierarchical radial layout to better visualize both transcription factor interactions and biosynthetic and metabolic pathways (Data S3). Screening for interacting gene products that are up- or down-regulated during low P conditions revealed several distinct families. Numerous auxin, autophagy, and photosynthetic genes show distinct regulatory patterns within the GRN, as do several genes involved in sulfur and cysteine metabolism. Two up-regulated cysteine-related metabolism and signaling genes in particular were SORBI_3008G179900 and SORBI_3001G427300, which encode an O-acetylserine (thiol) lyase (OAS-TL) and a glycosyl transferase, respectively. Prior research into hypomorphs of these orthologs have shown they are either associated with reduced root growth and root surface area, specifically within lateralization of roots or are essential for proper response to LP conditions (Mei et al., 2019; Okazaki et al., 2013; Wang et al., 2015). Upon examination of the enriched

peaks of H3K4me3 and H3K27me3 sequencing across the OAS-TL and transferase gene models, there is a noticeable enrichment for H3K4me3 peaks at the five prime genic or promoter region in both genes in LP or SP-grown plants (Figure S6), but there is a narrowing of the peak width under LP growth conditions.

3 | DISCUSSION

3.1 | BTx623 root responses to P deficiency stress

We observed that P starvation caused a rather drastic remodeling of root system morphology in BTx623. From 7 DAT to 14 DAT, under low P growth conditions, root system length, surface area and volume increased 250%, 235%, and 224%, respectively, compared with the same root traits for plants grown on sufficient P (Table 1). Furthermore, at 7 DAT there was no difference in average root diameter between the two P treatments, but by 14 DAT, root system diameter had decreased a moderate (14%) and statistically significant amount in LP versus SP grown plants. Increases in lateral root growth in response to P deficiency have been previously observed in other plants, for example, in beans (Lynch & Brown, 2001), *Arabidopsis* (Arrese-Igor et al., 2020), and tomato (Hai-Bo et al., 2001). These changes in root traits are consistent with P acquisition efficiency explaining most of the genetic variation in overall P efficiency in maize and sorghum (Bernardino et al., 2019; de Sousa et al., 2012; Parentoni et al., 2010; Parentoni & de Souza, 2008). Phosphorus uptake is hindered, in part, due to the phosphate anion interacting strongly with Al- and Fe-oxides on the surface of soil clay minerals, resulting in much of it being fixed in the soil. This chemical behavior between P and soil minerals results in P being the most diffusion limited of the essential mineral nutrients. Hence, plant developmental strategies that increase root proliferation in the soil to reduce the distance between roots and soil P in ways that reduce the carbon cost for producing more roots, such as generating finer roots that have a higher surface area to volume ratio, appear to be key aspects of P efficiency. Certainly, the root responses shown here for sorghum BTx623 are consistent with these strategies.

3.2 | Gene targets for crop P efficiency improvement

In a broad sense, the root transcriptome data presented in this study is consistent with prior investigations on the genes whose expression is significantly altered by P deficiency stress and are a resource for P efficiency candidate genes. These include transcription factors involved in root development, such as *SHORTROOT* (*SHR*), *SCARECROW* (*SCR*) and *ROOTLESS CONCERNING CROWN AND SEMINAL ROOTS* (*RTCS*), phosphate transporters, and genes associated with auxin signaling, response, and transport. The significant changes in gene expression induced by P deficiency primarily

in lateral root apices (compared with the primary root apical and subapical regions) depicted in Figure 2 correlate at the physiological level with the root system response to LP in Figure 1 and Table 1, where lateral root growth stimulation is the major P deficiency growth response.

When evaluating transcription factors that are strongly up- or down-regulated in the lateral and apical root regions, a biological process ontology analysis suggests that specific hormone shunting is occurring throughout the RSA, with a specific increase in auxin activation within the lateral roots, and a shared downregulation of auxin and ABA signaling possibly occurring in the root apex. There could also be an overlapping response that is generally believed to be a response to biotic stress but could also be involved in root low P responses. This biotic response that plays a role in modulating RSA in response to chitin, involves the downregulation of *WRKY* transcription factors (Data S1) that play roles in root responses to fungal chitins that alter RSA (Wang et al., 2019, 2020).

An interesting finding from the gene expression and histone marks data was the identification of multiple genes involved in sulfur and cysteine metabolism that were discovered through the generation of a lateral root GRN filtered for H3K4me3 peak enrichment and up-regulated expression in response to LP. The functional relevance of this finding is supported by previous work indicating that sulfur metabolic pathways are integral to auxin changes in the root apex, leading to enhanced lateral root growth (Li et al., 2015; Mei et al., 2019; Romero et al., 2014; Wang et al., 2015; Zhao et al., 2014). It is not surprising to find such links between regulatory networks for two different essential nutrients, in this case, P and S. Another example of such interactions comes from the growing evidence of cross talk and co-regulation between P and N homeostasis (Medici et al., 2019) provide evidence that the plant P starvation response is regulated in part by both local and long-distance N signaling pathways. Another fascinating regulatory interaction of essential mineral nutrients is the complex interplay and role of Fe transport, cellular compartmentation and metabolism in P deficiency-induced alterations in primary root growth (Balzergue et al., 2017; Mora-Macias et al., 2017; Müller et al., 2015).

The DNA and histone methylation footprints presented here agree with prior investigations into epigenetic profiles of genic regions as we found there was significant enrichment at the gene body for both K27me3 and K4me3, with a drop in DNA methylation over the same space (Peng et al., 2019; Regulski et al., 2013; Zhu et al., 2017). Specifically focusing on histone methylation, K4me3 levels in LP plants seemed to decrease significantly across the TSS, five prime UTR, and transcript-encoding components of gene, and while K27me3 levels also decreased across the same segments, it was not nearly to the same degree as K4me3 levels (~50% drop). Another distinct global histone methylation characteristic in response to LP was the increase in H3K4me3 levels in the intergenic space. This is contrasted with global intergenic H3K27me3 and DNA methylation levels that remained largely unchanged under LP versus SP treatments. Specifically, the spread of the H3K4me3/H3K27me3 ratio across intergenic regions became narrower under limiting phosphorus, more so at



loci proximal to transcriptional start sites (>1000 bp upstream). Additionally, it was observed that there are moderately weak positive correlations between gene transcription and H3K4me3 mark intensity at genic and promoter regions and weakly negative or negligible correlations with H3K27me3 mark intensity across the same intervals (data not shown; \sim .3–.4 spearman correlation values for transcript CPM compared with K4me3 ChIP-seq peaks and \sim -.1–.3 for H3K27me3 peaks). All of these findings suggest that such histone methylation patterns could play a role in overall phosphate starvation adaptation. Further investigations into the frequency and location of more open chromatin marks, such as H3 lysine acetylation, might reveal stronger correlations with gene expression. Additionally, it was discovered here that enriched sequences surrounding histone methylation sites and DNA hypomethylation regions included binding sequences for transcription factors known to be associated with root growth and response to environmental stimuli (Figure 4). When comparing these findings to the Arabidopsis limiting phosphorus epigenome study of Yong-Villalobos et al. (2015), consistencies are observed with higher rates of CG DMRs compared with CHG and CHH and with overall enrichment at different gene feature; intergenic space, promoters, and gene body space comprising the majority of the methylation marks. Disagreement with the Arabidopsis study appears when noting trends in hypermethylation versus hypomethylation: sorghum roots under limiting phosphorus show strong hypomethylated preference, compared with hypermethylated sites in Arabidopsis. These data suggest potentially divergent functional roles for DNA methylation signaling between the two species, with the understanding that the experimental designs are not perfect replications. These data set the stage for future investigations into promoter, enhancer, and cryptic sequence regulatory candidates that may play roles in the molecular basis for enhanced P efficiency, which could be used to improve crop adaptation to low P soils which are prevalent worldwide, limiting agricultural production especially in the developing world (Kochian, 2012; Lynch, 2011).

During a shift from growth on sufficient to low phosphorus conditions, there is a coordinated de-methylation in sorghum roots that occurs both at the K4 and K27 lysine in histone 3, along with a trend towards increases in hypomethylated DMRs for 5-methylcytosine DNA methylation. Specifically, K4me3 peaks at the genic and promoter regions have a mild positive correlation with gene expression. The shift in epigenetic regions containing K4me3, K27me3, or DNA methylation peaks in response to low P are enriched for numerous DNA-binding motifs recognized by several transcription factor families. Some of which are notably, AP2/ERF, NAC, WRKY, and LOB transcription factors that can play a role in downstream gene activation for numerous hormone signaling pathways, specifically auxin, as well as canonical PSI genes and shared nutrient response pathways (nitrogen and sulfur). These gene up-regulations seem to be localized predominantly to the lateral root region, suggesting that the primary transcriptomic remodeling of the RSA is focused within the lateral root apices, and that the RSA epigenetic shift likely supports these changes in RSA to maximize root growth in low soil phosphorus environments (Figure S7).

4 | CONCLUSIONS

Imposing phosphorus (P) deficiency stress induced significant changes in the root architecture of the *S. bicolor* reference cultivar, BTx623. These included a significant stimulation of lateral root growth, which resulted in increases in total root system length, root surface area and total root system volume. We used genomic and epigenetic approaches to investigate transcriptional and chromatin changes in response to these P deficiency-induced changes in root architecture, which enhance sorghum's ability to acquire P from the soil. Three distinct root regions were studied: the primary root apical and subapical regions, and the lateral root apical region. Intriguing transcriptional responses were seen, with the majority of the genes whose expression were significantly up- or down-regulated localized to the lateral root apex. Under LP growth conditions, the epigenetic profiles of DNA methylation and histone trimethylation also showed distinct changes both around gene models and especially in the intergenic space. Combined together, these data revealed unique epigenetic shifts under limiting nutrient conditions that were associated with genes that could influence root development, but also previously undiscovered candidate genes and regulatory motifs that could influence changes in sorghum RSA that enhances P acquisition from low P soils. Taken together, the transcriptomic and epigenetic data in this study are a resource for future research on sorghum and other related cereals for the ultimate purpose of generating improved crop PUE through, in part, root systems that are more efficient and effective at “mining” P from the soil.

5 | METHODS

5.1 | Plant growth conditions

5.1.1 | Sorghum growth protocols for epigenetic and genomic assays

Sorghum seeds were surface-sterilized in a solution of 6% (v/v) sodium hypochlorite for 15 min. The sodium hypochlorite was removed by washing the seeds with distilled water 5 times. The seeds were then germinated on filter paper moistened with water for 4 days. After that, uniformly growing seedlings were transferred to 200 liter polypropylene tubs grown hydroponically with aerated modified Magnavaca nutrient solution (see Magnavaca et al., 1987, for nutrient solution composition). For nutrient solution with sufficient P (SP), the phosphate concentration was 45 μ M and for low P (LP) the phosphate concentration used was 2.5 μ M. As the phosphate was added as KH_2PO_4 , to maintain the same K concentration in the LP media as in the SP media, the KCl concentration in the LP media was increased from 1 to 1.0425 mM (1042.5 μ M). The sides of the tub were covered with white light reflective plastic and the nutrient solution in each tub was covered with gray, closed-cell polyethylene foam strips (McMaster-Carr, Elmhurst, IL, USA) to prevent light penetration and support the seedlings during the experiment (Figure 1b). Plants were

grown under controlled conditions in an EGC walk-in growth chamber for the duration of the experiment (27°C day/22°C night, 12/12 h photoperiod, 500 mmol m⁻² s⁻¹). After 1 day in sufficient P nutrient solution, half of the seedlings were transferred to low phosphorus nutrient solution (LP) where the 45-μM KH₂PO₄ was replaced with 2.5-μM KH₂PO₄. The pH of the solution was maintained at the range of 5.6–5.7 by adjustment with .5-M NaOH or HCl every 2 days. The nutrient solution was renewed every 5 days. Each treatment had 3 biological replications. Plants were grown in SP and LP conditions and root tissue was harvested after 10 days of growth on LP or HP conditions, for preparation of the libraries described below.

5.1.2 | Sorghum plant growth for 2D RSA analysis

Sorghum seeds were surface sterilized and germinated as described above. After 4 days of germination, uniform sorghum seedlings were transplanted and grown hydroponically using the same modified Magnavaca nutrient solution described above except the phosphate concentration used for SP media was increased to 200 μM. As above, the pH of the solution was maintained at the range of 5.6–5.7 by adjustment with .5-M NaOH or HCl every 2 days. The nutrient solution was renewed every 2 days for the growth of the plants in the pouch system. Single sorghum seedlings were grown in specially designed and constructed acrylic chambers which hold the seedling and root system on the surface of filter paper (described in more detail below). These 2D root growth chambers were placed vertically into 100-L polypropylene tubs (L × W × H = 50 × 30 × 65 cm) containing aerated modified Magnavaca nutrient solution whose composition is given above. Aluminum rails attached to the longer sides of each tub allowed the growth pouches to hang into the nutrient solution in the tubs. The level of the aerated nutrient solution was adjusted so it always was just below the root apex of the fastest growing seminal root. Each container held 20 plants, each in their individual pouches. A cover is placed on top of and sides of the tubs allowing the shoot to grow while excluding light from the roots and the nutrient solution.

The plant growth pouches consist of several layers of different materials. On the bottom is a perforated plastic back that provides rigidity to the pouch and the holes in the plastic backing facilitate better nutrient and air exchange. On top of this plastic back were placed several layers of germination paper which provide the nutrient solution to the plant roots. On top of the germination paper is a single sheet of black filter paper (Black Qualitative Filter Paper, Ahlstrom Corp; VWR, Part of Avantor; <https://www.avantorsciences.com/pages/en/vwr-part-of-avantor>) that serves as an anchor for the roots as they grow across its surface, and the black background provides high contrast with the roots, greatly improving root imaging. Finally, a sheet of clear polyester film covers the root system and black filter paper, protecting the root system from drying out and also contributing to root system anchorage to the black filter paper during growth, maintaining the root systems two-dimensional architecture.

5.2 | Sorghum root imaging and analysis

At 7, 10, and 14 days after transplanting, individual pouches with one sorghum plant were removed from the hydroponic tub, the plastic film carefully removed, and the plant on the pouch system was carefully placed oriented horizontally in a glass tray containing water with the root system totally submerged in the water. The tray with plant was placed into a 2D root imaging platform consisting of a frame constructed from 80:20 aluminum rails, to which is attached a Nikon D7200 DSLR camera with a 50-mm lens. Also attached to the frame are flashlights with diffusers (soft boxes) to diffuse the illuminating light across the root system, preventing shadows that can compromise the quality of root images. The root systems are submerged in water to prevent any unwanted diffraction and reflection of the illuminating light.

Our Plant Root Imaging and Data Acquisition (PRIDA) program, which is a python-based image acquisition and data management software, was used for collecting and storing raw images and project meta-data into a single Hierarchical Data Format (HDF5) file (<https://www.hdfgroup.org>). Images were then extracted as TIFF image files for further processing and root trait computation. These TIFF images were then fed into commercial and publicly available software packages for root trait computation. These software packages process the images to segment the RSA and separate it from other background objects by using different techniques, such as global, local, or adaptive thresholding. The segmentation process provides a clean RSA and for the next step in the process, skeletonization, which provides a single pixel line to provide a skeleton of the RSA. This skeleton is used to estimate a range of root growth and architecture traits. WinRHIZO software (Regents Instruments, Inc) was used to quantify root growth and topology traits, and GiA Roots (Galkovskyi et al., 2012) was used to quantify 2D root architecture traits. Taken together, root topology and architecture traits including average root diameter (cm), primary root length (cm), root system width (cm), convex hull area (cm²), specific root length (cm/cm³), root system surface area (cm²), total root system length (cm), and total root system volume (cm³) were investigated in this study.

5.3 | RNA-seq library preparation and analysis

The first 2 cm of the seminal root tips were excised with razor blades, and then the next 2 cm of the same seminal roots were also excised, and both tissue samples were separately frozen in liquid N₂. Additionally, the first 2 cm of the lateral root tips were also excised with razor blades and frozen, and all three tissue samples were used for preparation of the different libraries described here and below. Root tip samples were collected from both SP and LP grown plants, after 10 days of growth in SP and LP media. The lateral roots emerged starting after about 5 days of growth and we collected root tips from all lateral roots that were at least 5 cm in length (as roots shorter than 5 cm roots were quite thin and hard to cut). We excised and collected the 2 cm long root tips from approximately the 20 longest lateral roots on



each plant and these lateral roots were approximately 3–5 days in age. We collected root samples from the one seminal root and approximately the 20 longest lateral roots. The root samples from 10 plants constituted one biological replicate.

Root tissue samples were ground in liquid nitrogen and then the RNA was isolated in Trizol reagent (ThermoFisher) followed by purification using Zymo-spin columns (Directzol RNA kit; Zymo Research). Column-bound RNA was treated with DNase 1 and finally eluted with 50 μ l of DNase/RNase-free water. RNA quality was determined using the Bioanalyzer hardware with the Agilent RNA 6000 Nano Kit (Agilent). Poly-A RNA was isolated from total RNA using Dynabeads (ThermoFisher). Libraries for sequencing were created using the ScriptSeq RNA-seq prep kit (Illumina) following manufacturer protocols. Final libraries were amplified with 17 cycles of PCR and assessed on the Bioanalyzer with the High Sensitivity DNA kit (Agilent). All root tissue libraries that were sequenced comprised two biological replicates.

Sequencing platform information. Sequencing was performed at Cold Spring Harbor Laboratories using the Illumina HiSeq2000 platform with 100 bp paired-end reads. Paired-end fastq files were trimmed for quality with Trimmomatic and then merged with Samtools before aligning to the v3.4.1 *S. bicolor* genome with Kallisto package in rStudio v3.6.1. Differential gene expression was determined through DESeq2 after importing Kallisto abundance files with tximport package. Dimensional analysis was performed using the factoextra package. Heatmaps and hierarchical clustering were performed with the heatmap.2 package in rStudio.

The phosphate starvation Induced (PSI) gene set was derived from the Yong-Villalobos et al. (2015) manuscript. See Data S2.

5.4 | ChIP-seq library preparation and analysis

The entire root systems were harvested for ChIP-seq library preparation. The root tissue was cut into sections and fixed in 10-mM dimethyl adipimate (DMA; Sigma-Aldrich) while applying a vacuum. Samples were ground in liquid nitrogen and then placed in extraction buffer, filtered through miracloth and then a 30-mm CellTrics filter (CellTrics). Nuclei were isolated and then chromatin was sheared in 130-ml tubes (Covaris). Shearing was performed on a Covaris S220 sonicator for 5 min at a cycle/burst of 200, peak power of 175, and duty factor of 10. Immunoprecipitation was performed with antibodies for H3K27me3 (Millipore), H3K4me3 (Abcam), H3 (Abcam) for input control, and Protein A Dynabeads (ThermoFisher) for input control. Crosslinking was reversed and samples were purified using Chip DNA Clean and Concentrator Kit (Zymo Research). Libraries were created using the Nextflex ChIP-Seq library prep kit (Bioo Scientific) with the NextFlex ChIP-seq Barcodes. Sequencing was done on a HiSeq 2500 v4 with 125 bp paired-end reads. Paired-end fastq files were trimmed for quality with Trimmomatic and then mapped to the v3.4.1 *S. bicolor* genome with BWA (bwa mem -q 30, -f 2 -ubhS). Sorted bam files were marked for duplicates with Picard and then merged with Samtools. Tag directories creation and peak calling, peak enrichment comparison was performed through the Homer package.

Overlapped peaks were identified through Bedtools (intersectBed). Peak annotation was performed using the annotatePeaks module of the Homer software. Samtools was used to obtain flagstat metrics and perform various file conversion and handling. Various visualization and file creation was performed using the deepTools package (Ramírez et al., 2016); aligned bam files (that were input-controlled) were converted to bigWig format for generating computeMatrix files for plotHeatmap and plotEnrichment outputs. *k*-means cluster number was determined by selecting the result that generated the distinct read coverage within and around gene models while minimizing cluster overlap.

5.5 | Bisulfite-seq library preparation and analysis

Bisulfite-sequencing was done as described in (Li et al., 2014). The root apices (first two cm) of all primary and lateral roots were excised from plants grown as described above after 10 days of growth on SP and LP media. The root samples from 10 plants constituted one biological replicate.

DNA was isolated from root sections and sheared into fragments between 200 and 300 bp in length. These fragments underwent end repair, dA tailing, and ligation to methylated adaptors for subsequent bisulfite conversion. Libraries were PCR amplified, purified, and quality controlled via Agilent DNA 1000 chip. Sequencing was done on a HiSeq 2500 v4 with 125 bp paired-end reads. Reads were trimmed and quality controlled using Trim Galore and FASTQC respectively (<http://www.bioinformatics.babraham.ac.uk/projects/index.html>). Reads were aligned and extracted with Bismark (Krueger & Andrews, 2011). Differential methylation quantification and visualizations were done with MethylKit (Akalin et al., 2012). Additional visualizations were performed with deepTools (Ramírez et al., 2016) after converting Bismark-aligned bam files to bigWig and then generating computeMatrix files for plotHeatmap and plotEnrichment outputs.

5.6 | GRN analysis

All available protein–protein interaction data was gathered from the STRING v11 database (Szklarczyk et al., 2018) for genes that have an affiliated K4me3 peak at their genic or promoter region, as annotated by Homer AnnotatePeaks. This phosphate responsive root GRN was organized in a hierarchical radial layout in Cytoscape v3.8.2 to better visualize both transcription factor interactions and biosynthetic and metabolic pathways (Shannon et al., 2003). Gene nodes were then colorized for the RNA-seq log₂ fold change from the lateral root region.

5.7 | Additional analysis and tools

DNA motif analysis for all sequencing data was performed by the MEME suite using the ANR method, minimum motif width of six, and

an e-value threshold of less than or equal to 0.01. Assorted data handling and manipulation was performed with Samtools (Li et al., 2009), Bedtools (Quinlan & Hall, 2010), and UCSC software packages (Kent et al., 2010). Genome browser views were carried out with the Integrated Genome Viewer software (Robinson et al., 2011).

ACKNOWLEDGMENTS

We would like to thank Jon Shaff for their assistance in growing the sorghum plants and helping isolate root tissue for the RNA-seq and epigenetic assays. We would like to thank Robert Martienssen and the Martienssen laboratory for discussions and feedback on the epigenetic assays. This research was supported by funding from a Canada Excellence Research Chairs (CERC) grant to LVK, funding from the Global institute for Food Security, University of Saskatchewan to LVK. Funding from United States Department of Agriculture, USDA-ARS 8062-21000-041-00D to DW. We acknowledge support from the Embrapa Macroprogram, the Fundação de Amparo à Pesquisa do Estado de Minas Gerais (FAPEMIG), and the National Council for Scientific and Technological Development (CNPq) to JM.

CONFLICT OF INTEREST

The authors claim no conflict of interest.

AUTHOR CONTRIBUTIONS

LK, JM, and DW contributed to the experimental design. BH, JM, ZL, and LK grew the sorghum plants and collected the root tissue samples for library preparation. JM and MR generated the sequencing libraries. NG and XW performed bioinformatic and statistical analyses; NG wrote the manuscript. All authors contributed to the manuscript writing and editing process.

DATA AVAILABILITY STATEMENT

Sequencing data are available on the National Center for Biotechnology Information Sequence Read Archive (NCBI SRA: <https://www.ncbi.nlm.nih.gov/sra>). BioProject ID for sequencing files is PRJNA454504.

ORCID

Nicholas Gladman  <https://orcid.org/0000-0002-9000-8377>

Barbara Hufnagel  <https://orcid.org/0000-0002-3515-2122>

Leon Kochian  <https://orcid.org/0000-0003-3416-089X>

Jurandir Magalhães  <https://orcid.org/0000-0002-6673-6497>

Doreen Ware  <https://orcid.org/0000-0002-8125-3821>

REFERENCES

- Akalin, A., Kormaksson, M., Li, S., Garrett-Bakelman, F. E., Figueroa, M. E., Melnick, A., & Mason, C. E. (2012). methylKit: A comprehensive R package for the analysis of genome-wide DNA methylation profiles. *Genome Biology*, 13, R87. <https://doi.org/10.1186/gb-2012-13-10-r87>
- Arrese-Igor, S., Alegría, A., Arbe, A., & Colmenero, J. (2020). Insights into the Non-exponential Behaviour of the Dielectric Debye-like Relaxation in Monoalcohols. arXiv [physics.chem-ph] 312 113441 <https://doi.org/10.1016/j.molliq.2020.113441>
- Balzerque, C., Dartevelle, T., Godon, C., Laugier, E., Meisrimler, C., Teulon, J.-M., Creff, A., Bissler, M., Brouchoud, C., Hagège, A., Müller, J., Chiarenza, S., Javot, H., Becuwe-Linka, N., David, P., Péret, B., Delannoy, E., Thibaud, M.-C., Armengaud, J., ... Thierry, D. (2017). Low phosphate activates STOP1-ALMT1 to rapidly inhibit root cell elongation. *Nature Communications*, 8, 15300. <https://doi.org/10.1038/ncomms15300>
- Barros, V. A., Chandnani, R., de Sousa, S. M., Maciel, L. S., Tokizawa, M., Guimaraes, C. T., Magalhães, J. V., & Kochian, L. V. (2020). Root adaptation via common genetic factors conditioning tolerance to multiple stresses for crops cultivated on acidic tropical soils. *Frontiers in Plant Science*, 11, 565339. <https://doi.org/10.3389/fpls.2020.565339>
- Bayuelo-Jiménez, J. S., Gallardo-Valdéz, M., Pérez-Decelis, V. A., Magdaleno-Armas, L., Ochoa, I., & Lynch, J. P. (2011). Genotypic variation for root traits of maize (*Zea mays* L.) from the Purhepecha plateau under contrasting phosphorus availability. *Field Crops Res*, 121, 350–362. <https://doi.org/10.1016/j.fcr.2011.01.001>
- Bellini, C., Pacurar, D. I., & Perrone, I. (2014). Adventitious roots and lateral roots: Similarities and differences. *Annual Review of Plant Biology*, 65, 639–666. <https://doi.org/10.1146/annurev-arplant-050213-035645>
- Bernardino, K. C., Pastina, M. M., Menezes, C. B., de Sousa, S. M., Maciel, L. S., Carvalho, G. Jr., Guimarães, C. T., Barros, B. A., da Costa E Silva, L., Carneiro, P. C. S., Schaffert, R. E., Kochian, L. V., & Magalhães, J. V. (2019). The genetic architecture of phosphorus efficiency in sorghum involves pleiotropic QTL for root morphology and grain yield under low phosphorus availability in the soil. *BMC Plant Biology*, 19, 87. <https://doi.org/10.1186/s12870-019-1689-y>
- Calderón-Vázquez, C., Alatorre-Cobos, F., Simpson-Williamson, J., & Herrera-Estrella, L. (2009). Maize under phosphate limitation. In JL Bennetzen, SC Hake, eds, *Handbook of maize: Its biology*. Springer New York, pp 381–404. https://doi.org/10.1007/978-0-387-79418-1_19
- Chen, D.-H., Huang, Y., Jiang, C., & Si, J.-P. (2018). Chromatin-based regulation of plant root development. *Frontiers in Plant Science*, 9, 1509. <https://doi.org/10.3389/fpls.2018.01509>
- Cooper, E. A., Brenton, Z. W., Flinn, B. S., Jenkins, J., Shu, S., Flowers, D., Luo, F., Wang, Y., Xia, P., Barry, K., Daum, C., Lipzen, A., Yoshinaga, Y., Schmutz, J., Saski, C., Vermerris, W., & Kresovich, S. (2019). A new reference genome for *Sorghum bicolor* reveals high levels of sequence similarity between sweet and grain genotypes: Implications for the genetics of sugar metabolism. *BMC Genomics*, 20, 420. <https://doi.org/10.1186/s12864-019-5734-x>
- Cordell, D., Drangert, J.-O., & White, S. (2009). The story of phosphorus: Global food security and food for thought. *Glob Environ Change*, 19, 292–305. <https://doi.org/10.1016/j.gloenvcha.2008.10.009>
- Cordell, D., & White, S. (2013). Sustainable phosphorus measures: Strategies and technologies for achieving phosphorus security. *Agronomy*, 3, 86–116. <https://doi.org/10.3390/agronomy3010086>
- Dai, X., Wang, Y., Yang, A., & Zhang, W.-H. (2012). OsMYB2P-1, an R2R3 MYB transcription factor, is involved in the regulation of phosphate-starvation responses and root architecture in rice. *Plant Physiology*, 159, 169–183. <https://doi.org/10.1104/pp.112.194217>
- de Sousa, S. M., Clark, R. T., Mendes, F. F., de Oliveira, A. C., de Vasconcelos, M. J. V., Parentoni, S. N., Kochian, L. V., Guimarães, C. T., & Magalhães, J. V. (2012). A role for root morphology and related candidate genes in P acquisition efficiency in maize. *Functional Plant Biology*, 39, 925–935. <https://doi.org/10.1071/FP12022>
- de Wet, J. M. J., & Huckabay, J. P. (1967). The origin of *Sorghum bicolor*. II. Distribution and domestication. *Evolution*, 21, 787–802. <https://doi.org/10.1111/j.1558-5646.1967.tb03434.x>



- Deng, X., Song, X., Wei, L., Liu, C., & Cao, X. (2016). Epigenetic regulation and epigenomic landscape in rice. *National Science Review*, 3, 309–327. <https://doi.org/10.1093/nsr/nww042>
- Devaiah, B. N., Nagarajan, V. K., & Raghothama, K. G. (2007). Phosphate homeostasis and root development in Arabidopsis are synchronized by the zinc finger transcription factor ZAT6. *Plant Physiology*, 145, 147–159. <https://doi.org/10.1104/pp.107.101691>
- Dillon, S. L., Shapter, F. M., Henry, R. J., Cordeiro, G., Izquierdo, L., & Lee, L. S. (2007). Domestication to crop improvement: Genetic resources for sorghum and Saccharum (Andropogoneae). *Annals of Botany*, 100, 975–989. <https://doi.org/10.1093/aob/mcm192>
- Doumbia, M. D., Hossner, L. R., & Onken, A. B. (1993). Variable sorghum growth in acid soils of subhumid West Africa. *Arid Soil Research and Rehabilitation*, 7, 335–346. <https://doi.org/10.1080/15324989309381366>
- Doumbia, M. D., Hossner, L. R., & Onken, A. B. (1998). Sorghum growth in acid soils of West Africa: Variations in soil chemical properties. *Arid Soil Research and Rehabilitation*, 12, 179–190.
- Galkovskiy, T., Mileyko, Y., Bucksch, A., Moore, B., Symonova, O., Price, C. A., Topp, C. N., Iyer-Pascuzzi, A. S., Zurek, P. R., Fang, S., Harer, J., Benfey, P. N., & Weitz, J. S. (2012). GiA Roots: software for the high throughput analysis of plant root system architecture. *BMC Plant Biology*, 12, (1), <https://doi.org/10.1186/1471-2229-12-116>
- Gamuyao, R., Chin, J. H., Pariasca-Tanaka, J., Pesaresi, P., Catausan, S., Dalid, C., Slamet-Loedin, I., Tecson-Mendoza, E. M., Wissuwa, M., & Heuer, S. (2012). The protein kinase Pstol1 from traditional rice confers tolerance of phosphorus deficiency. *Nature*, 488, 535–539. <https://doi.org/10.1038/nature11346>
- Hai-Bo, L. I., Ming, X. I. A., & Ping, W. U. (2001). Effect of phosphorus deficiency stress on rice lateral root growth and nutrient absorption. *Journal of Integrative Plant Biology*, 43, 1154–1160.
- Hu, B., Zhu, C., Li, F., Tang, J., Wang, Y., Lin, A., Liu, L., Che, R., & Chu, C. (2011). LEAF TIP NECROSIS1 plays a pivotal role in the regulation of multiple phosphate starvation responses in rice. *Plant Physiology*, 156, 1101–1115. <https://doi.org/10.1104/pp.110.170209>
- Hufnagel, B., de Sousa, S. M., Assis, L., Guimaraes, C. T., Leiser, W., Azevedo, G. C., Negri, B., Larson, B. G., Shaff, J. E., Pastina, M. M., Barros, B. A., Weltzien, E., Rattunde, H. F. W., Viana, J. H., Clark, R. T., Falcão, A., Gazaffi, R., Garcia, A. A. F., Schaffert, R. E., ... Magalhães, J. V. (2014). Duplicate and conquer: Multiple homologs of PHOSPHORUS-STARVATION TOLERANCE1 enhance phosphorus acquisition and sorghum performance on low-phosphorus soils. *Plant Physiology*, 166, 659–677. <https://doi.org/10.1104/pp.114.243949>
- Kent, W. J., Zweig, A. S., Barber, G., Hinrichs, A. S., & Karolchik, D. (2010). BigWig and BigBed: Enabling browsing of large distributed datasets. *Bioinformatics*, 26, 2204–2207. <https://doi.org/10.1093/bioinformatics/btq351>
- Khan, G. A., Vogiatzaki, E., Glauser, G., & Poirier, Y. (2016). Phosphate deficiency induces the jasmonate pathway and enhances resistance to insect herbivory. *Plant Physiology*, 171, 632–644. <https://doi.org/10.1104/pp.16.00278>
- Kochian, L. V. (2012). Plant nutrition: Rooting for more phosphorus. *Nature*, 488, 466–467. <https://doi.org/10.1038/488466a>
- Krueger, F., & Andrews, S. R. (2011). Bismark: A flexible aligner and methylation caller for bisulfite-Seq applications. *Bioinformatics*, 27, 1571–1572. <https://doi.org/10.1093/bioinformatics/btr167>
- Leiser, W. L., Rattunde, H. F. W., Weltzien, E., Cisse, N., Abdou, M., Diallo, A., Touré, A. O., Magalhães, J. V., & Haussmann, B. I. G. (2014). Two in one sweep: Aluminum tolerance and grain yield in P-limited soils are associated to the same genomic region in West African sorghum. *BMC Plant Biology*, 14, 206. <https://doi.org/10.1186/s12870-014-0206-6>
- Li, H., Handsaker, B., Wysoker, A., Fennell, T., Ruan, J., Homer, N., Marth, G., Abecasis, G., Durbin, R., & 1000 Genome Project Data Processing Subgroup. (2009). The sequence alignment/map format and SAMtools. *Bioinformatics*, 25, 2078–2079. <https://doi.org/10.1093/bioinformatics/btp352>
- Li, Q., Eichten, S. R., Hermanson, P. J., Zaunbrecher, V. M., Song, J., Wendt, J., Rosenbaum, H., Madzima, T. F., Sloan, A. E., Huang, J., Burgess, D. L., Richmond, T. A., McGinnis, K. M., Meeley, R. B., Danilevskaia, O. N., Vaughn, M. W., Kaepler, S. M., Jeddeloh, J. A., & Springer, N. M. (2014). Genetic perturbation of the maize methylome. *Plant Cell*, 26, 4602–4616. <https://doi.org/10.1105/tpc.114.133140>
- Li, X., Huang, L., Hong, Y., Zhang, Y., Liu, S., Li, D., Zhang, H., & Song, F. (2015). Co-silencing of tomato S-adenosylhomocysteine hydrolase genes confers increased immunity against pseudomonas syringae pv. Tomato DC3000 and enhanced tolerance to drought stress. *Frontiers in Plant Science*, 6, 717. <https://doi.org/10.3389/fpls.2015.00717>
- Li, Z., Xu, C., Li, K., Yan, S., Qu, X., & Zhang, J. (2012). Phosphate starvation of maize inhibits lateral root formation and alters gene expression in the lateral root primordium zone. *BMC Plant Biology*, 12, 89. <https://doi.org/10.1186/1471-2229-12-89>
- López-Arredondo, D. L., Leyva-González, M. A., González-Morales, S. I., López-Bucio, J., & Herrera-Estrella, L. (2014). Phosphate nutrition: Improving low-phosphate tolerance in crops. *Annual Review of Plant Biology*, 65, 95–123. <https://doi.org/10.1146/annurev-arplant-050213-035949>
- López-Bucio, J., Hernández-Abreu, E., Sánchez-Calderón, L., Nieto-Jacobo, M. F., Simpson, J., & Herrera-Estrella, L. (2002). Phosphate availability alters architecture and causes changes in hormone sensitivity in the Arabidopsis root system. *Plant Physiology*, 129, 244–256. <https://doi.org/10.1104/pp.010934>
- Lynch, J. P. (2011). Root phenes for enhanced soil exploration and phosphorus acquisition: Tools for future crops. *Plant Physiology*, 156, 1041–1049. <https://doi.org/10.1104/pp.111.175414>
- Lynch, J. P., & Brown, K. M. (2001). Topsoil foraging: An architectural adaptation of plants to low phosphorus. *Plant and Soil*, 237, 225–237. <https://doi.org/10.1023/A:1013324727040>
- MacDonald, G. K., Bennett, E. M., Potter, P. A., & Ramankutty, N. (2011). Agronomic phosphorus imbalances across the world's croplands. *Proceedings of the National Academy of Sciences of the United States of America*, 108, 3086–3091. <https://doi.org/10.1073/pnas.1010808108>
- Magnavaca, R., Gardner, C. O., & Clark, R. B. (1987). Inheritance of aluminum tolerance in maize. In W. H. Gabelman & B. C. Loughman (Eds.), *Genetic aspects of plant mineral nutrition: Proceedings of the second international symposium on genetic aspects of plant mineral nutrition, organized by the University of Wisconsin, Madison, June 16–20, 1985* (pp. 201–212). Springer Netherlands. https://doi.org/10.1007/978-94-009-3581-5_18
- McCormick, R. F., Truong, S. K., Sreedasyam, A., Jenkins, J., Shu, S., Sims, D., Kennedy, M., Amirebrahimi, M., Weers, B. D., McKinley, B., Mattison, A., Morishige, D., Grimwood, J., Schmutz, J., & Mullet, J. E. (2018). The Sorghum bicolor reference genome: Improved assembly, gene annotations, a transcriptome atlas, and signatures of genome organization. *The Plant Journal*, 93, 338–354. <https://doi.org/10.1111/tpj.13781>
- Medici, A., Szponarski, W., Dangeville, P., Safi, A., Dissanayake, I. M., Saenchai, C., Emanuel, A., Rubio, V., Lacombe, B., Ruffel, S., Tanurdzic, M., Rouached, H., & Krouk, G. (2019). Identification of molecular integrators shows that nitrogen actively controls the phosphate starvation response in plants. *Plant Cell*, 31, 1171–1184. <https://doi.org/10.1105/tpc.18.00656>
- Mei, Y., Zhao, Y., Jin, X., Wang, R., Xu, N., Hu, J., Huang, L., Guan, R., & Shen, W. (2019). L-cysteine desulfhydrase-dependent hydrogen

- sulfide is required for methane-induced lateral root formation. *Plant Molecular Biology*, 99, 283–298. <https://doi.org/10.1007/s11103-018-00817-3>
- Miller, C. R., Ochoa, I., Nielsen, K. L., Beck, D., & Lynch, J. P. (2003). Genetic variation for adventitious rooting in response to low phosphorus availability: Potential utility for phosphorus acquisition from stratified soils. *Functional Plant Biology*, 30, 973–985. <https://doi.org/10.1071/FP03078>
- Mora-Macías, J., Ojeda-Rivera, J. O., Gutiérrez-Alanis, D., Yong-Villalobos, L., Oropeza-Aburto, A., Raya-González, J., Jiménez-Domínguez, G., Chávez-Calvillo, G., Rellán-Álvarez, R., & Herrera-Estrella, L. (2017). Malate-dependent Fe accumulation is a critical checkpoint in the root developmental response to low phosphate. *Proceedings of the National Academy of Sciences*, 114, E3563–E3572. <https://doi.org/10.1073/pnas.1701952114>
- Müller, J., Toev, T., Heisters, M., Teller, J., Moore, K. L., Hause, G., Dinesh, D. C., Bürstenbinder, K., & Abel, S. (2015). Iron-dependent callose deposition adjusts root meristem maintenance to phosphate availability. *Developmental Cell*, 33, 216–230. <https://doi.org/10.1016/j.devcel.2015.02.007>
- Nguyen, H. N., Kim, J. H., Jeong, C. Y., Hong, S.-W., & Lee, H. (2013). Inhibition of histone deacetylation alters Arabidopsis root growth in response to auxin via PIN1 degradation. *Plant Cell Reports*, 32, 1625–1636. <https://doi.org/10.1007/s00299-013-1474-6>
- Okazaki, Y., Otsuki, H., Narisawa, T., Kobayashi, M., Sawai, S., Kamide, Y., Kusano, M., Aoki, T., Hirai, M. Y., & Saito, K. (2013). A new class of plant lipid is essential for protection against phosphorus depletion. *Nature Communications*, 4, 1510. <https://doi.org/10.1038/ncomms2512>
- Parentoni, S. N., & de Souza, C. L. Jr. (2008). Phosphorus acquisition and internal utilization efficiency in tropical maize genotypes. *Pesqui Agropecu Bras*, 43, 893–901. <https://doi.org/10.1590/S0100-204X2008000700014>
- Parentoni, S. N., de Souza, C. L. Jr., de Carvalho Alves, V. M., Gama, E. E. G., Coelho, A. M., de Oliveira, A. C., Guimarães, P. E. O., Guimarães, C. T., Vasconcelos, M. J. V., Patto Pacheco, C. A., Meirelles, W. F., de Magalhães, J. V., Moreira Guimarães, L. J., da Silva, A. R., Ferreira Mendes, F., & Schaffert, R. E. (2010). Inheritance and breeding strategies for phosphorus efficiency in tropical maize (*Zea mays* L.). *Maydica*, 55, 1.
- Park, B. S., Seo, J. S., & Chua, N.-H. (2014). NITROGEN LIMITATION ADAPTATION recruits PHOSPHATE2 to target the PHOSPHATE transporter PT2 for degradation during the regulation of Arabidopsis PHOSPHATE homeostasis. *Plant Cell*, 26, 454–464. <https://doi.org/10.1105/tpc.113.120311>
- Paterson, A. H., Bowers, J. E., Bruggmann, R., Dubchak, I., Grimwood, J., Gundlach, H., Haberler, G., Hellsten, U., Mitros, T., Poliakov, A., Schmutz, J., Spannagl, M., Tang, H., Wang, X., Wicker, T., Bharti, A. K., Chapman, J., Feltus, F. A., Gowik, U., ... Rokhsar, D. S. (2009). The *Sorghum bicolor* genome and the diversification of grasses. *Nature*, 457, 551–556. <https://doi.org/10.1038/nature07723>
- Peng, Y., Xiong, D., Zhao, L., Ouyang, W., Wang, S., Sun, J., Zhang, Q., Guan, P., Xie, L., Li, W., Li, G., Yan, J., & Li, X. (2019). Chromatin interaction maps reveal genetic regulation for quantitative traits in maize. *Nature Communications*, 10, 2632. <https://doi.org/10.1038/s41467-019-10602-5>
- Péret, B., Desnos, T., Jost, R., Kanno, S., Berkowitz, O., & Nussaume, L. (2014). Root architecture responses: In search of phosphate. *Plant Physiology*, 166, 1713–1723. <https://doi.org/10.1104/pp.114.244541>
- Quinlan, A. R., & Hall, I. M. (2010). BEDTools: A flexible suite of utilities for comparing genomic features. *Bioinformatics*, 26, 841–842. <https://doi.org/10.1093/bioinformatics/btq033>
- Ramírez, F., Ryan, D. P., Grüning, B., Bhardwaj, V., Kilpert, F., Richter, A. S., Heyne, S., Dündar, F., & Manke, T. (2016). deepTools2: A next generation web server for deep-sequencing data analysis. *Nucleic Acids Research*, 44, W160. <https://doi.org/10.1093/nar/gkw257>
- Regulski, M., Lu, Z., Kendall, J., Donoghue, M. T. A., Reinders, J., Llaça, V., Deschamps, S., Smith, A., Levy, D., McCombie, R., Tingey, S., Rafalski, A., Hicks, J., Ware, D., & Martienssen, R. A. (2013). The maize methylome influences mRNA splice sites and reveals widespread paramutation-like switches guided by small RNA. *Genome Research*, 23, 1651–1662. <https://doi.org/10.1101/gr.153510.112>
- Robinson, J. T., Thorvaldsdóttir, H., Winckler, W., Guttman, M., Lander, E. S., Getz, G., & Mesirov, J. P. (2011). Integrative genomics viewer. *Nature Biotechnology*, 29, 24–26. <https://doi.org/10.1038/nbt.1754>
- Romero, L. C., Aroca, M. Á., Laureano-Marín, A. M., Moreno, I., García, I., & Gotor, C. (2014). Cysteine and cysteine-related signaling pathways in Arabidopsis thaliana. *Molecular Plant*, 7, 264–276. <https://doi.org/10.1093/mp/sst168>
- Schulze, J., Temple, G., Temple, S. J., Beschow, H., & Vance, C. P. (2006). Nitrogen fixation by white lupin under phosphorus deficiency. *Annals of Botany*, 98, 731–740. <https://doi.org/10.1093/aob/mcl154>
- Shannon, P., Markiel, A., Ozier, O., Baliga, N. S., Wang, J. T., Ramage, D., Amin, N., Schwikowski, B., & Ideker, T. (2003). Cytoscape: A software environment for integrated models of biomolecular interaction networks. *Genome Research*, 13, 2498–2504. <https://doi.org/10.1101/gr.1239303>
- Shi, J., Dong, A., & Shen, W.-H. (2014). Epigenetic regulation of rice flowering and reproduction. *Frontiers in Plant Science*, 5, 803.
- Smith, A. P., Jain, A., Deal, R. B., Nagarajan, V. K., Poling, M. D., Raghoothama, K. G., & Meagher, R. B. (2010). Histone H2A.Z regulates the expression of several classes of phosphate starvation response genes but not as a transcriptional activator. *Plant Physiology*, 152, 217–225. <https://doi.org/10.1104/pp.109.145532>
- Szklarczyk, D., Gable, A. L., Lyon, D., Junge, A., Wyder, S., Huerta-Cepas, J., Simonovic, M., Doncheva, N. T., Morris, J. H., Bork, P., Jensen, L. J., & von Mering, J. (2018). STRING v11: Protein–protein association networks with increased coverage, supporting functional discovery in genome-wide experimental datasets. *Nucleic Acids Research*, 47, D607–D613.
- Thibaud, M.-C., Arrighi, J.-F., Bayle, V., Chiarenza, S., Creff, A., Bustos, R., Paz-Ares, J., Poirier, Y., & Nussaume, L. (2010). Dissection of local and systemic transcriptional responses to phosphate starvation in Arabidopsis. *The Plant Journal*, 64, 775–789. <https://doi.org/10.1111/j.1365-3113.2010.04375.x>
- Wang, C., Tariq, R., Ji, Z., Wei, Z., Zheng, K., Mishra, R., & Zhao, K. (2019). Transcriptome analysis of a rice cultivar reveals the differentially expressed genes in response to wild and mutant strains of *Xanthomonas oryzae* pv. *Oryzae*. *Scientific Reports*, 9, 3757. <https://doi.org/10.1038/s41598-019-39928-2>
- Wang, H.-L., Yang, S.-H., Lv, M., Ding, S.-W., Li, J.-Y., Xu, C.-L., & Xie, H. (2020). RNA-Seq revealed that infection with white tip nematodes could downregulate rice photosynthetic genes. *Functional & Integrative Genomics*, 20, 367–381. <https://doi.org/10.1007/s10142-019-00717-9>
- Wang, Z., Mao, J.-L., Zhao, Y.-J., Li, C.-Y., & Xiang, C.-B. (2015). L-cysteine inhibits root elongation through auxin/PLETHORA and SCR/SHR pathway in Arabidopsis thaliana. *Journal of Integrative Plant Biology*, 57, 186–197. <https://doi.org/10.1111/jipb.12213>
- West, P. T., Li, Q., Ji, L., Eichten, S. R., Song, J., Vaughn, M. W., Schmitz, R. J., & Springer, N. M. (2014). Genomic distribution of H3K9me2 and DNA methylation in a maize genome. *PLoS ONE*, 9, e105267. <https://doi.org/10.1371/journal.pone.0105267>
- Yong-Villalobos, L., González-Morales, S. I., Wrobel, K., Gutiérrez-Alanis, D., Cervantes-Peréz, S. A., Hayano-Kanashiro, C., Oropeza-Aburto, A., Cruz-Ramírez, A., Martínez, O., & Herrera-Estrella, L.



- (2015). Methylome analysis reveals an important role for epigenetic changes in the regulation of the Arabidopsis response to phosphate starvation. *Proceedings of the National Academy of Sciences of the United States of America*, 112, E7293–E7302. <https://doi.org/10.1073/pnas.1522301112>
- Zhao, Q., Wu, Y., Gao, L., Ma, J., Li, C.-Y., & Xiang, C.-B. (2014). Sulfur nutrient availability regulates root elongation by affecting root indole-3-acetic acid levels and the stem cell niche. *Journal of Integrative Plant Biology*, 56, 1151–1163. <https://doi.org/10.1111/jipb.12217>
- Zhou, J., Jiao, F., Wu, Z., Li, Y., Wang, X., He, X., Zhong, W., & Wu, P. (2008). OsPHR2 is involved in phosphate-starvation signaling and excessive phosphate accumulation in shoots of plants. *Plant Physiology*, 146, 1673–1686. <https://doi.org/10.1104/pp.107.111443>
- Zhou, P., Li, Z., Magnusson, E., Gomez Cano, F., Crisp, P. A., Noshay, J. M., Grotewold, E., Hirsch, C. N., Briggs, S. P., & Springer, N. M. (2020). Meta gene regulatory networks in maize highlight functionally relevant regulatory interactions. *Plant Cell*, 32, 1377–1396. <https://doi.org/10.1105/tpc.20.00080>
- Zhu, A., Greaves, I. K., Dennis, E. S., & Peacock, W. J. (2017). Genome-wide analyses of four major histone modifications in Arabidopsis hybrids at the germinating seed stage. *BMC Genomics*, 18, 137. <https://doi.org/10.1186/s12864-017-3542-8>

SUPPORTING INFORMATION

Additional supporting information may be found in the online version of the article at the publisher's website.

How to cite this article: Gladman, N., Hufnagel, B., Regulski, M., Liu, Z., Wang, X., Chougule, K., Kochian, L., Magalhães, J., & Ware, D. (2022). Sorghum root epigenetic landscape during limiting phosphorus conditions. *Plant Direct*, 6(5), e393. <https://doi.org/10.1002/pld3.393>